

Hysteresis, force oscillations and non-equilibrium effects in the adhesion of spherical nanoparticles to atomically smooth surfaces

German Drazer^{†,*}, Boris Khusid[§], Joel Koplik[‡], and Andreas Acrivos[†]

[†] *Benjamin Levich Institute, City College of the City University of New York, New York, NY 10031*

[§] *Department of Mechanical Engineering, New Jersey Institute of Technology, University Heights, Newark, NJ 07102 and*

[‡] *Benjamin Levich Institute and Department of Physics, City College of the City University of New York, New York, NY 10031*

(Dated: November 21, 2018)

Abstract

Molecular dynamics simulations are used to examine hysteretic effects and distinctions between equilibrium and non-equilibrium aspects of particle adsorption on the walls of nano-sized fluid-filled channels. The force on the particle and the system's Helmholtz free energy are found to depend on the particle's history as well as on its radial position and the wetting properties of the fluid, even when the particle's motion occurs on time scales much longer than the spontaneous adsorption time. The hysteresis is associated with changes in the fluid density in the gap between the particle and the wall, and these structural rearrangements persist over surprisingly long times. The force and free energy exhibit large oscillations with distance when the lattice of the structured nanoparticle is held in register with that of the tube wall, but not if the particle is allowed to rotate freely. Adsorbed particles are trapped in free energy minima in equilibrium, but if the particle is forced along the channel the resulting stick-slip motion alters the fluid structure and allows the particle to desorb.

PACS numbers: 47.15.Gf,47.11.+j,47.15.Rq,68.08.-p

Keywords: nanochannel,molecular dynamics,adhesion,hysteresis

The behavior of fluids in confined geometries with characteristic length scales in the nanometer range has received enormous attention in recent years. Among the motivations for such *nanofluidic* studies is the development of controlled fabrication techniques for materials at this scale, and their potential application to “lab-on-a-chip” devices [1] which could perform analyses of biochemical species at the single-molecule level [2]. Obviously, understanding the transport of suspended nanometer-size particles under microscopic confinement is a crucial ingredient in achieving the potential benefits of integrated nanofluidic systems. Atomistic numerical simulations have provided invaluable insight into the behavior of fluids under nanoconfinement, and have illustrated some dramatic phenomena not present in macroscopic hydrodynamics [3]. In previous work we used molecular dynamics (MD) simulations to study the transport of closely-fitting nanometer-size particles driven through a fluid-filled nanochannel, and observed a sharp transition between steady transport and spontaneous adsorption of the suspended particles, as a function of the solid-fluid interaction strength [4, 5]. Even for the computationally-efficient Lennard-Jones interactions used in that work, we were severely limited in the time scales accessible to simulation to values $\lesssim 0.1 \mu s$, and extrapolation to operational, laboratory time scales is somewhat uncertain. It would be very desirable therefore to develop multi-scale simulation techniques to bridge this gap, and to this end we study here the same adhesion phenomena from a thermodynamic perspective, exploring the free energy and fluid configurational changes associated with the adsorption of nanoparticles. The free energy is particularly relevant to mesoscale calculational methods such as phase field models and dissipative particle dynamics.

In fact, we observe substantial hysteresis in the Helmholtz free energy of the system when a nanoparticle executes a controlled adsorption/desorption cycle, even over times much larger than the time scale of the natural phenomena. The underlying mechanism appears to be the long-lived structural rearrangements of the fluid molecules in the gap region between the particle and the wall, in particular a delay in replenishing fluid in the gap between the wall and a receding particle. The persistence of this retarded condensation is quite surprising in a liquid with such simple short-ranged interactions. Since the free energy is a state variable, in the thermodynamic limit it should not exhibit hysteresis, and our results raise qualms about the conventional assumption of local thermodynamic equilibrium in most continuum modeling. In addition to hysteresis, nanoscale particle forces often exhibit oscillations as a function of radial position, and we observe that their presence depends on the ability of the

particle to rotate as it approaches the wall. Oscillations are present when the underlying lattice of the structured particles has a fixed orientation relative to that of the tube wall, but not if the particle is allowed to rotate freely. Lastly, we compare the desorption of the particle from the wall in equilibrium and non-equilibrium situations: in equilibrium there is a substantial free energy barrier to particle release, whereas if the particle is driven parallel to the wall it is more likely to detach.

The MD simulations are based on an atomistic description of a fluid interacting via Lennard-Jones potentials, $V_{LJ}(r) = 4\epsilon [(r/\sigma)^{-12} - A(r/\sigma)^{-6}]$, where r is the interatomic separation, σ is roughly the size of the repulsive core, of order a few angstroms, and will be used as the length scale, ϵ is the strength of the potential (and the energy unit), and A is a dimensionless parameter that controls the attraction between the various atomic species and thus determines the wetting properties of the system [6]. The corresponding characteristic time scale, $\tau = \sqrt{m\sigma^2/\epsilon}$, where m is the mass of the fluid atoms, is a few picoseconds. A Nosé-Hoover thermostat is used to fix the temperature of the system at $T = 1.0\epsilon/k_B$, with k_B the Boltzmann constant. Further technical details of the simulations may be found in [5]. The fluid is confined to a cylindrical channel, whose walls are composed of atoms of mass $m_w = 100m$, tethered by a stiff linear spring to fixed lattice sites obtained from a cylindrical section of an fcc lattice with lattice constant $\ell = 1.71$ corresponding to a wall number density $\rho_w = 0.8$. (Length of the tube: $L_x = 34.20$. Inner and outer radii: $R = 10.26$ and $R_o = 16.25$) The spherical nanoparticle is constructed in an analogous fashion using a spherical section of radius $a = 5.13$. The atoms in the particle are, however, fixed at the lattice sites, allowing the motion of the nanoparticle to be computed by rigid body dynamics, integrating Newton's and Euler's equations. Finally, to avoid a perfect matching in the underlying structures of both solids the equilibrium position of each atom is perturbed by a small random displacement [5]. The particle and channel wall are made of the same material and their atoms interact via the LJ potential with $A = 1$. The fluid atoms also interact among themselves with the $A = 1$ standard LJ potential and the volume-average number density is the same as that of the tube wall, $\rho_{av} = 0.8$, which, at $T = 1.0$, corresponds to the fluid phase of the Lennard-Jones bulk system, slightly above the critical temperature.

In our previous work, we applied an axial force to the particle, and observed a sudden spontaneous transition from statistically steady motion parallel to the tube axis to

adsorption on the walls, when the strength of the solid-fluid van der Waals attraction falls below a critical value $A_c \simeq 0.8$ (for both spherical and ellipsoidal particles). Here, we first measure the changes in the Helmholtz free energy \mathcal{F} of the system as the sphere *quasi-statically* approaches the wall in the radial direction and then recedes to its original position at the center of the tube, by performing a thermodynamic integration. The free energy difference between any two points during this switching process is then given by $\mathcal{F}(r) - \mathcal{F}(0) = W = \int_0^r \langle F(\lambda) \rangle d\lambda$, where W is the work done on the system and $\langle F \rangle$ is the radial force acting on the particle at radius λ , averaged over an ensemble of 10 statistically independent realizations, and over a time interval t_s . Specifically, the center of mass of the sphere is translated at constant velocity in the radial direction, typically over a distance $\Delta r = 0.01$ in time $t_s = 50$ ($u = 2 \times 10^{-4} \sim 1\text{cm/s}$), then held in place for a further time interval t_s , then translated again. First, we consider the case where the sphere is allowed to rotate freely in the suspending fluid at all times. The time average is meant as a substitute for an ensemble average, assuming ergodicity, with the (modest) ensemble average is meant to compensate for any peculiarities in the initial configuration.

In Fig. 1 we show the average force on the sphere as a function of its radial position, for various degrees of wetting, $A = 0.6, 0.8$ and 1.0 , which exhibits large hysteresis as $A \rightarrow 1$. On the other hand, we found no hysteresis, even at relatively large approaching velocities, for the $A = 0$ case of a completely non-wetting fluid. (An isolated fluid drop with this interaction would float off a solid wall.) The inset to Fig. 1 compares, for one case, the average force during the translation step to that when the sphere is held in place, and the agreement between the two values indicates that the observed hysteresis is not due to drag or other irreversible forces arising from the motion of the sphere, in spite of the relatively large approaching speed ($u \sim 10\text{cm/s}$) used in this comparison. In Fig. 2 we present the Helmholtz free-energy of the system, together with the potential energy, for the same values of A . The adsorption/desorption hysteresis is clear in the $A > 0$ cases, with the work needed to separate the particles from the wall clearly higher than the gain in free-energy from bringing the particles in contact with the wall, *i. e.*, $W > 0$. This result shows that the adhesion process is generally a non-equilibrium process that dissipates energy. On the other hand, we observe that the potential energy of the system (sum of all LJ interactions) does not display any significant hysteresis. In addition, a detailed study of each of the separate contributions shows that the energy increase observed for $r \gtrsim 5.0$ in the wetting

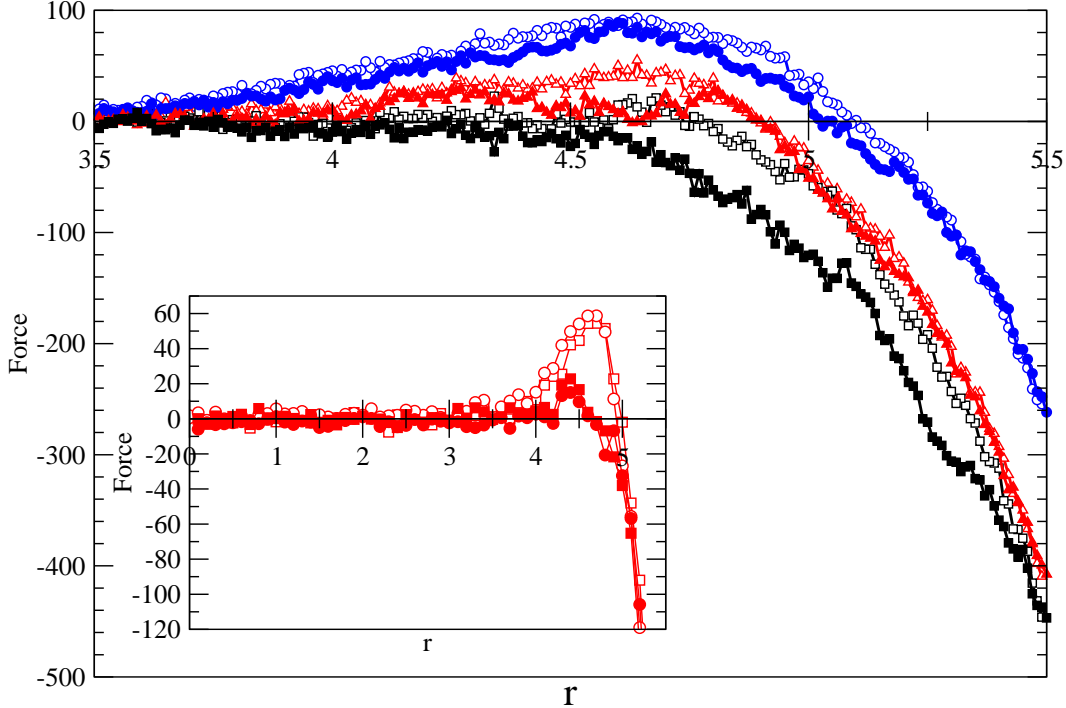


FIG. 1: Average force on the spherical particles during the adsorption/desorption cycles as a function of the radial position for $A = 0.6$ (circles), $A = 0.8$ (triangles), and $A = 1$ (squares). The solid (open) symbols correspond to the approaching (receding) part of the cycle. The approaching velocity is $u \sim 1\text{cm/s}$. The inset shows, for the case $A = 0.8$, the average force measured during radial motion (squares) and in a stationary radial position (circles) for an overall approaching speed of $u \sim 10\text{cm/s}$.

case $A = 1$ results from the deformation of the wall as the particle pushes against it, rather than structural or solvation effects.

We have performed simulations at different approach speeds and for different wetting conditions and, although $W > 0$ in all $A > 0$ cases, the hysteresis is reduced as the characteristic times become larger, as shown in the inset to Fig. 2. This is expected, since the process should be reversible with $W = 0$ if it were to be carried out infinitely slowly [7]. It is important to note, however, that the motion of the sphere in these simulations is very slow compared with the natural time scale of the spontaneous process. Indeed, the characteristic time for the approaching and receding parts of the free energy measurements is roughly $2.5 \times 10^4 \tau$, an order of magnitude larger than typical adsorption times observed when a sphere is freely suspended. (See, for example, the estimate of the diffusive time to reach the

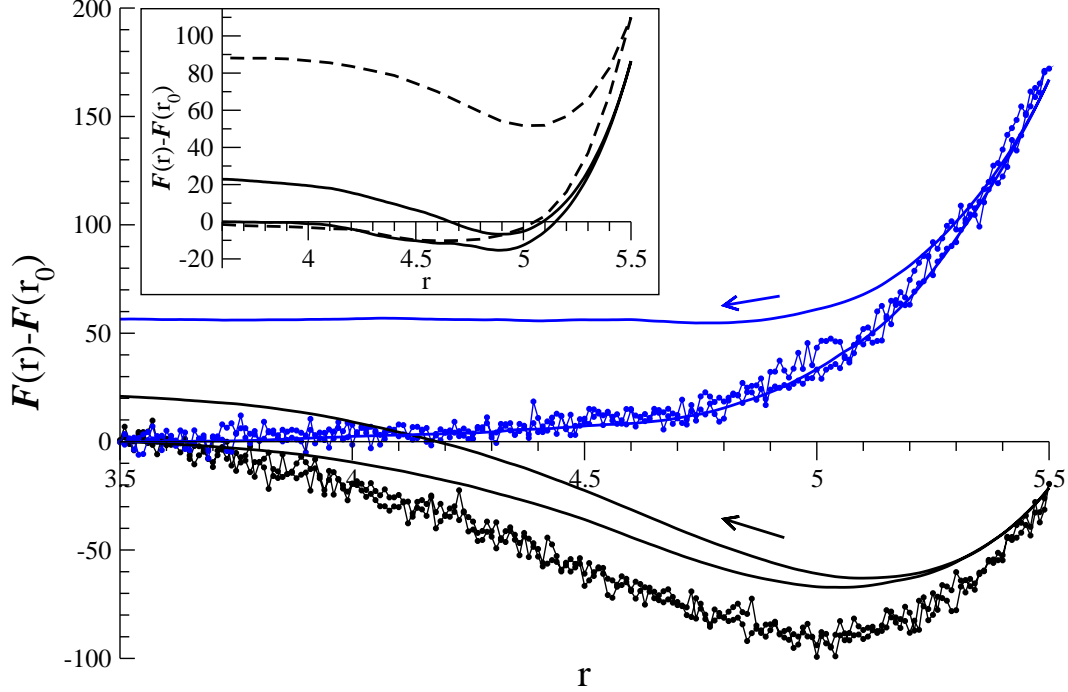


FIG. 2: Free-energy and potential-energy differences as a function of the radial position of the spherical particle for $A = 0.6$ (bottom curves) and $A = 1$ (top curves). The points correspond to the potential energy of the system evaluated from the interparticle interactions. The solid line corresponds to the free-energy calculated during the adsorption/desorption cycle (an arrow indicates the curve corresponding to the receding part of the measurement.) The inset shows the free-energy differences computed for $A = 0.8$ at two different approaching velocities, $u \sim 10\text{cm/s}$ (dashed lines) and $u \sim 1\text{cm/s}$ (solid line).

wall, $\tau_D \sim 2500\tau$, and the numerical results in Table II for $A = 0.6$, in Ref. [5].)

The molecular mechanism underlying the hysteresis appears to be the history-dependence of the number of particles in the gap between the sphere and the tube wall, for gap sizes of the order of the diameter of a single fluid molecule. In Fig. 3 we see that the number of gap particles during the desorption branch is smaller, corresponding to a depletion of particles relative to the bulk density. The absence of fluid leads to the dominance of the attractive wall-particle interactions and depletion forces, explaining the results presented in Fig. 1, including the surprising result obtained for $A = 0.80$ at $u \sim 10\text{cm/s}$, in which the force on the sphere is repulsive when approaching the wall but attractive in the pull-off measurements (see the inset to Fig. 1). The dependence of hysteresis on the degree of wetting of the fluid

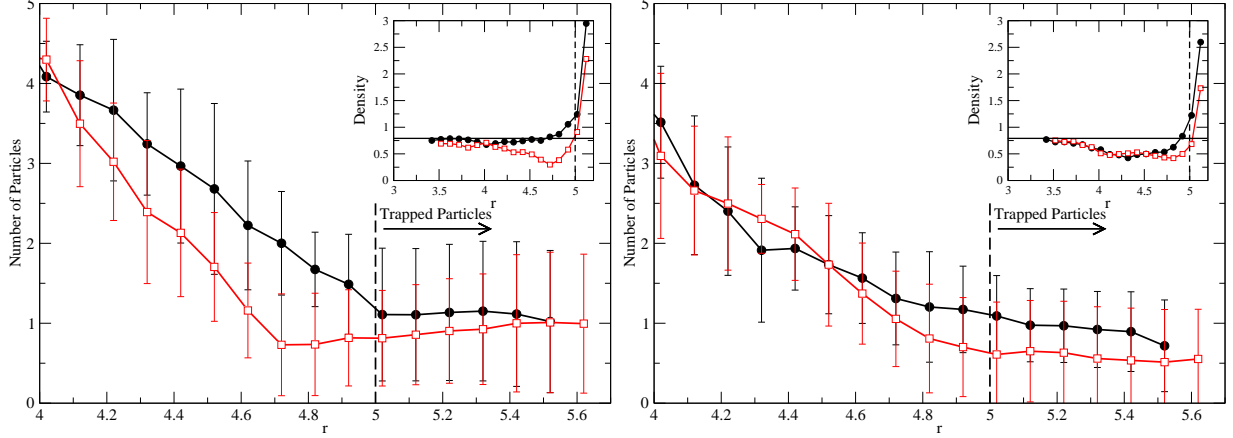


FIG. 3: Average number of fluid molecules in the particle-wall gap during the adsorption/desorption cycles for $A = 0.85$. The number of particles is tracked in a cylindrical region of radius $a/4$ between the sphere and the tube surfaces, and the corresponding number density is given in the insets. The solid (open) symbols correspond to the approaching (receding) branch and the dashed line marks the radial position at which the volume of the cylindrical region is less than the volume of a single fluid molecule. The top (bottom) figure corresponds to $u \sim 10$ cm/s ($u \sim 1$ cm/s).

may be understood in terms of the relative ease of pushing fluid atoms out of the gap region, which obviously improves as the fluid becomes less wetting. Furthermore, the presence of a nearly-planar wall induces layering and presumably other structural correlations within the fluid, which can contribute to hysteresis if any significant time is required for the structure to reestablish itself after the particle is pulled away. Again, this effect is reduced as $A \rightarrow 0$. Lastly, we note from Fig. 3 that the hysteresis in the number of gap particles decreases substantially as the approach velocity is reduced, consistent with the presumption that it would be absent in the limit of infinitesimally slow approach.

Somewhat analogous hysteretic behavior due to fluid depletion has been seen in a study of cavitation by Bolhuis and Chandler [8], who measured the force between non-wetting parallel plates which approach and recede while immersed in a Lennard-Jones liquid. These authors consider a WCA potential, whose behavior one would expect to be similar to our $A = 0$ case, but other operating conditions differ in that the bulk density and temperature are much lower, while the plate velocity is much higher. In rough agreement with our results, force hysteresis is not observed at the highest temperature studied, $T = 0.81\epsilon/k_B$, but does

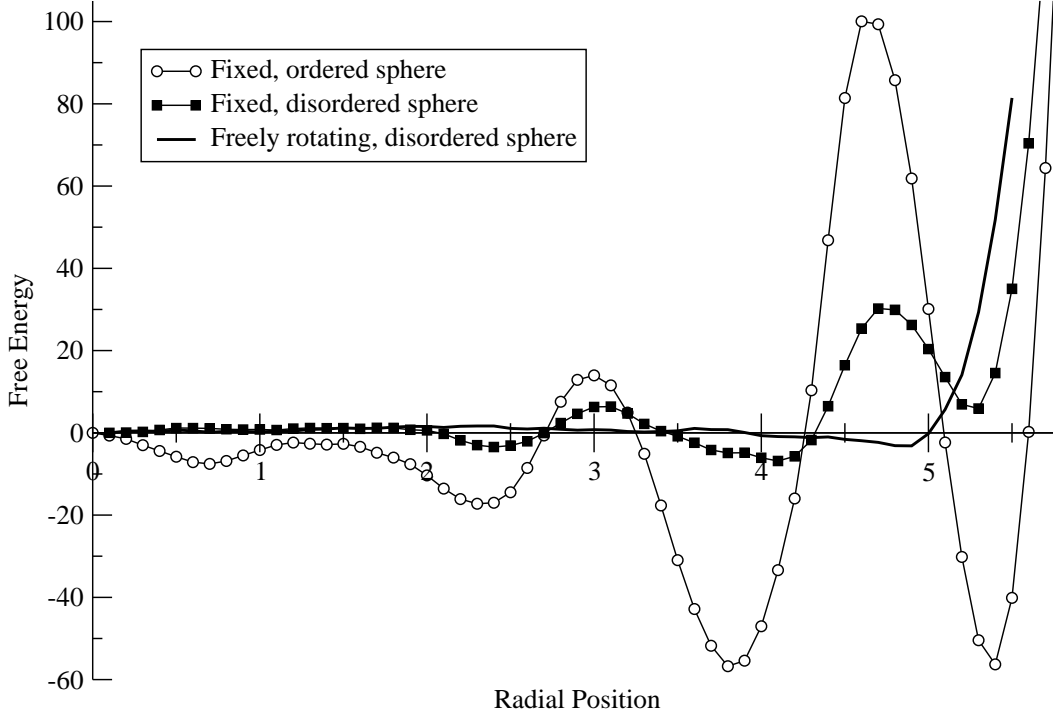


FIG. 4: Free-energy differences as a function of the radial position of the spherical particle for $A = 1$. The open (closed) symbols correspond to an ordered (disordered) sphere with fixed orientation approaching an ordered (disordered) tube wall. The solid line corresponds to the disordered sphere rotating freely.

appear at lower temperatures, perhaps as a result of glassy behavior. In the latter cases, there are high and low density states in the gap between plates with the high density state apparently metastable, and the hysteresis is attributed to a retardation in the (non)wetting-induced cavitation inside the gap.

A notable feature of the density profiles in Fig. 3 is that the particles leave the gap *continuously*, without a noticeable effect on the solvation layers known to occur close to solid surfaces [7, 9, 10]. The smoothness of this transition is in agreement with the absence of oscillatory solvation forces in the measurements presented in Fig. 1. This effect results from the ability of the particle to rotate freely as it approaches the wall, and indicates that a freely suspended particle might overcome solvation force barriers that prevent strong adhesion, by adjusting its atomic lattice orientation relative to that of the wall. In Fig. 4 we show the results of an alternate simulation at $A = 1$ where the orientation of the particle is fixed during its slow motion towards the wall, which does exhibit the familiar oscillations as layers of fluid

are successively squeezed out of the gap region. In contrast, in the freely rotating case the structured particles have some freedom to avoid close approach to a particular fluid atom by a rotation of their atomic lattice, leading to a gradual displacement of fluid atoms, in contrast to the fixed case where the approaching particle uniformly displaces fluid away from itself. Furthermore, when the particle is very close to the wall, its orientation tends to lock into values determined by the nearly solid wall structure. Note that the disorder introduced in the position of the solid atoms is smaller than the atomic diameter of the fluid atoms and should not destroy the molecular ordering of the fluid close to the wall [7] and in fact density oscillations are observed in our system [5]. The same argument applies to the curvature of the tube wall. In fact, we also show in fig. 4 that, although substantially reduced compared to the ordered case, oscillatory solvation forces are still present for disordered solids.

The particle desorption process also exhibits some important physical distinctions depending on whether the particle is left alone in equilibrium or is subject to continued forcing, as in [4, 5]. We see in Fig. 2 that, for partially-wetting fluids ($A < 1$), a particle close to the wall is confined by a substantial potential barrier, roughly $40\epsilon/k_B$ (for $A = 0.8$ and $u \sim 1\text{cm/s}$), and is unlikely to spontaneously desorb under the action of equilibrium fluctuations alone. However, in our previous study of a driven particle motion we observed a spontaneous desorption of particles whenever $A \gtrsim 0.8$, which would indicate a much smaller pull-off force. The distinction is that desorption only occurs in non-equilibrium simulations in which a large external force is applied to the particles ($F \sim \text{pN}$). Note however that the effect is indirect, since the force is not radial but is instead in the direction of the tube axis. As found previously, axial forcing of the particle induces stick-slip motion along the wall after adsorption, which enhances dramatically both the mean and rms fluctuation in the number of atoms in the gap region, from a value of 2.0 ± 0.9 while in equilibrium to 7.0 ± 2.9 when the particle is forced along the wall. Related to this, adsorbed spheres undergoing stick-slip motion present comparatively large fluctuations in their radial position. A possible mechanism for desorption is that the sphere encounters ordered clusters of fluid molecules as it moves intermittently along the wall, which provide an (inward) radial fluctuation to a position where the wall attraction is reduced.

The results in this paper underline some of the issues arising when particle dynamics at the nanoscale are examined in quantitative detail. The results pose some challenges for the long-term goal of modifying the continuum description of particle-fluid dynamics to describe

phenomena at these length scales, since for example there is no single unique potential of mean force which may be incorporated. One immediate avenue for further study, would be to explore the validity of the number of particles in the gap as an order parameter for a multi-scale description.

This work was supported by the Engineering Research Program, office of Basic Energy Sciences, U. S. Department of Energy under Grant No. DE-FG02-03ER46068.

* Electronic address: drazer@mailaps.org

- [1] H. A. Stone, A. D. Stroock, and A. Ajdari, *Annu. Rev. Fluid Mech.* **36**, 381 (2004).
- [2] J. W. Hong and S. R. Quake, *Nature Biotech.* **21**, 1179 (2003).
- [3] O. Beckstein and M. S. P. Sansom, *Proc. Nat. Acad. Sci.* **100**, 7063 (2003).
- [4] G. Drazer, J. Koplik, A. Acrivos, and B. Khusid, *Phys. Rev. Lett.* **89**, 244501 (2002).
- [5] G. Drazer, J. Koplik, A. Acrivos, and B. Khusid, *Phys. Fluids* **17**, 017102 (2005).
- [6] J. L. Barrat and L. Bocquet, *Phys. Rev. Lett.* **82**, 4671 (1999).
- [7] J. N. Israelachvili, *Surf. Sci. Rep.* **14**, 109 (1992).
- [8] P. G. Bolhuis and D. Chandler, *J. Chem. Phys.* **113**, 8154 (2000).
- [9] P. M. McGuiggan and J. N. Israelachvili, *Chem. Phys. Lett.* **149**, 469 (1988).
- [10] Y. Qin and K. A. Fichtorn, *J. Chem. Phys.* **119**, 9745 (2003).